Static balancing of planar articulated robots

Static Balancing of Planar Articulated Robots

Giuseppe. Quaglia, Zhe. Yin
Department of Mechanical and Aerospace Engineering, Politecnico di Torino,
Corso Duca degli Abruzzi 24, 10129, Torino, Italy

Abstract: static balancing for a manipulator's weight is necessary in terms of energy saving and performance improvement. This paper proposes a method to design balancing devices for articulated robots in industry, based on robotic dynamics. Full design details for the balancing system using springs are presented from two aspects. One is the optimization for the position of the balancing system. The other is the design of the spring parameters. As examples, two feasible balancing devices are proposed, based on different robotic structures. The first solution consists of linkages and springs. The other consists of pulleys, cross mechanisms and (hydro-) pneumatic springs. Then the two solutions are compared. Pneumatic, hydro-pneumatic and mechanical springs are discussed and their parameters are decided according to the requirements of torque compensation. Numerical results show that with the proper design using the methodology presented in this paper, an articulated robot can be statically balanced perfectly in all configurations. This paper therefore provides a design method of the balancing system for other similar structures.

Keyword: Robotics; Static Balancing; Pneumatic Spring; Mechanical Spring; Torque Compensation;

Nomenclature

m_i	mass of Link i, kg	E_e	elastic potential energy
h_i	height of gravity centre of Link i, m	E_g	gravitational potential energy
θ_i	rotational angle of Link i, rad	$\dot{\theta}_i$	angular velocity of Link i, rad/s
$\ddot{\theta}_i$	angular acceleration of Link i, rad/s^2	g	gravitational acceleration, 9.8m/s^2
h_i	height of center of mass G_i, m	b_i	connecting link length, m
l_i	length of Link i, m	b_{iF}	arm of moment, m
r_i	distance between the two points	G_i	gravity of Link i, N
F_i	spring force, N	k_i	stiffness of spring i, N/m
C_i	torque from link mass and position, N*m	a_i	spring length between fixes joint and connecting link i
α_i	angle to locate the fixed joint for spring	δ_i	shift angle, rad
C_F	torque applied by balancing system, N*m	e	error
C_M	torque applied by Motor i (M_i), N*m	I_i	moment of inertia, referred to Joint O_i, kg*m^2
A_1	effective area, m^2	x_1	position of piston, m
V_{aux}	volume of auxiliary bladder, m^3	V	volume of pneumatic spring, m^3
P	pressure of pneumatic spring, Pa		

Subscripts

1	Link 1	2	Link 2
0	initial condition, θ=0	F	feasible constant force
Fk	feasible variable force	id	ideal

Corresponding author, email:giuseppe.quaglia@polito.it

c	torque	max	maximum
c%	torque error in percentage	c%mean	a mean value for torque error in percentage

1. Introduction

Energy saving has become increasingly important in recent years [1]. Especially in mechanical field, the issue reducing energy consumption is considered by designers of mechanical systems as a principal aspect. In industrial robotics, serial manipulators have a wide range of applications. Since they normally have massive links, which require extra actuator efforts, much research has been done to decrease energy consumption ([2][3][4]). Static balancing is a feasible technology to realize the energy saving target and many mechanical systems need to be equipped with balancing devices ([5][6][7]). A statically balanced system can move within its workspace in an energy-saving way.

Counter weights and springs are well-known tools to balance the gravity of mechanical systems in terms of energy saving. The counter-weight method shows many applications [2][3] due to its easy accessibility, however, at the same time, it introduces an undesirable increase in system inertia. Spring balancing avoids the disadvantage because of its low mass. Using auxiliary devices, such as parallelogram linkages or pulleys, a spring device normally can be designed in good connection with a mechanical system ([9]-[13]). If a design of a balancing device is done based on a good investigation of a system's structure, perfect equilibration can be realized in which the gravity effect of a system (with a balancing device in it) can be eliminated by the system itself [10]. Any configuration of the system will be statically balanced under a perfect equilibrating situation without spending energy from any actuator to keep its equilibrium.

Many research works have been done in the field of spring balancing with outstanding results ([4][7][8][14]-[24][28]-[37]). Kurt Hain [14] showed graphical methods about design of springs in his work. A linear spring was assumed and produced an oppositely equal torque to balance a gravity torque from a load or a manipulator at several positions. In his force analysis, a balancing-torque function was described as a variable of the device position angle ϕ and two springs were applied to replace an original one. Other ways to balance a load with a common pulley and a differential pulley were also illustrated in details. For point balancing where only few discrete points (less than five points) with known load torques needed to be balanced accurately, two methods were demonstrated in graphics. The fixed point for the spring connection was obtained by graphic 'trial and error'. For other positions, only approximate balancing was realized. For continuous balancing, an odd-convex pulley was designed according to a required variation of force arms. This way can provide precise balancing moments. Ion Simionescu and Liviu Ciupitu [15][16] discussed many ways to balance gravity of vertical and horizontal links with helical springs in their works. With an anthropomorphic structure, physical parameters describing a mechanism were collected for optimizing equations. More than a perfect balancing configuration were found since the optimal relationship has multi-solutions. In other configurations, approximate balancing was realized. With a cam mechanism, on the other hand, perfect balancing was managed in all workspace. An outline of a cam was designed to compensate errors due to non-linearity of energy change. Since the special outline of a cam is difficult to be manufactured, therefore perfect balancing with the cam is restricted to theoretical study. Bruzzone and Bozzini [4] applied a torsional spring to balance an articulated robot. They examined and discussed the influence from different stiffness and preload angles. The mechanism balanced with a torsional spring can reduce the energy consumption dramatically. Agrawal and Abbas Fattah ([17]-[19]) concluded a general theory to balance anthropomorphic robots. They classified static balancing problems into three categories according to different connecting joints: prismatic, revolute and spherical joints. They later studied balancing

strategies using springs for different joints. After locating centres of robotic systems with parallelograms, springs were designed to connect to the centres and to make the total potential energy of the systems invariant in all configurations. Then, based on an energy conservation principle, spring stiffness was calculated using physical parameters of the systems. S. Segla and R. Saravanan et al. [7][8] discussed optimization problems about physical parameters of the 'APR20' robot. In their papers, the 'APR20' robot was balanced by mean of springs. For the optimization of balancing effect in whole workspace, an objective function was built to describe an average force on a gripper. Then, all parameters were analysed with mathematic strategies such as a genetic algorithm, the Monte Carlo method. Finally, a compromise among parameters was selected for minimizing the value of the objective function.

Normally these works ([9]-[13], [17]-[20]) firstly show a combination of a balancing device and a mechanical model in their works, but present little information about how the combination is gradually built and developed. Among the works, authors follow the same methodology to realize the balancing target, based on the energy analysis: after investigating mechanisms with the spring balancer, gravitational and elastic potential energies are expressed in equations respectively. Then, to satisfy an assumption that the total potential energy is kept invariant, spring stiffness is obtained and examples are added to support conclusions. Unlike these works mentioned above, this paper tries to present another method to realize the balancing target, based on robotic dynamics. Then, balancing devices are designed from two aspects. One aspect discusses the position to place balancing systems. The other aspect refers to the design of spring parameters. With a combination of the two aspects, the perfect balance can be realized.

This paper is organised as follows: the methodology is presented in Section 2. The robotic dynamics is demonstrated for the balancer design. Two steps about designing a balancing system follow. Then, two structures of an articulated robot widely applied in industry are shown as study objects in Section 3. For the first structure, the balancing system with linkages and springs is introduced and discussed from two aspects. One focuses on the choice of positions for the balancing system and another is for spring design. The perfect torque compensation is realized and illustrated with numerical examples. For the second structure, a balancing system with pulleys, cross mechanisms and pneumatic springs is proposed. As a constant force generation device, pneumatic and hydro-pneumatic springs are applied. Finally, in Section 4, comparison between the two robotic structures is made. Conclusions and future work are also mentioned.

2. Methodology

This section demonstrates the methodology for the design of the balancing system. Robotic dynamics is introduced. The design target is to develop a balancing system which can produce the proper torque and counteract the gravity torque of the robot. The external motors in the balanced system do not compensate the gravity torque of the robot, therefore, they can save energy. Two design aspects based on the theory are considered. The one is to design and place a balancer to satisfy the torque requirements and the other is to decide the spring parameters to produce the matched spring forces.

2.1 Robotic dynamics

It is well known that the matrix equation describing robotic dynamics ([21][25]) is,

$$\mathbf{C} - \left[\mathbf{I}(\boldsymbol{\theta})\ddot{\boldsymbol{\theta}} + \mathbf{q}\left(\boldsymbol{\theta}, \dot{\boldsymbol{\theta}}\right) + \mathbf{G}(\boldsymbol{\theta})\right] = \mathbf{0} \tag{1}$$

Where **C** is the column vector of actuator torques, **I** is the manipulator inertia matrix, **q** is from kinetic effect. The gravity effect **G** is a non-linear function and the objective of gravity compensation. The aim of designing a balancing device is to reduce or eliminate the gravity effect during the workspace of the robot model.

For a non-balanced robot, actuators should actively supply all torques to counteract every item in Eq. (1). In this case, **C** can be assumed consisting of two components, $\mathbf{C_a}$ and $\mathbf{C_b}$. $\mathbf{C_a}$ is assumed to be the torque component to counteract the system's inertia **I** and kinetic effect **q**, while $\mathbf{C_b}$ is assumed to be the component to counteract the gravity effect **G**,

$$\begin{cases} \mathbf{C_a} = [\mathbf{I}(\boldsymbol{\theta})\ddot{\boldsymbol{\theta}} + \mathbf{q}(\boldsymbol{\theta}, \dot{\boldsymbol{\theta}})] \\ \mathbf{C_b} = \mathbf{G}(\boldsymbol{\theta}) \end{cases}$$

For a balanced robot, $\mathbf{C_b}$ can be replaced by a passive compensator. In this case, the introduction of the passive compensator can reduce or eliminate the consumption of actuator torques for the gravity effect item. If it happens, assuming that the torque from the passive compensator is $\mathbf{C_s}$, it is known,

$$\begin{cases} \mathbf{C_a} = [\mathbf{I}(\boldsymbol{\theta})\ddot{\boldsymbol{\theta}} + \mathbf{q}(\boldsymbol{\theta}, \dot{\boldsymbol{\theta}})] \\ \mathbf{C_s} = \mathbf{G}(\boldsymbol{\theta}) \\ \mathbf{C_b} = \mathbf{0} \end{cases}$$

In this way, actuators only need to supply the torque $\mathbf{C_a}$, therefore, the total energy consumption is saved. Eq. (1) can be evolved as,

$$\mathbf{C_a} - [\mathbf{I}(\boldsymbol{\theta})\ddot{\boldsymbol{\theta}} + \mathbf{q}(\boldsymbol{\theta}, \dot{\boldsymbol{\theta}})] + \mathbf{C_s} - \mathbf{G}(\boldsymbol{\theta}) = \mathbf{0} \quad (2)$$

The passive compensator producing $\mathbf{C_s}$ is the balancing device we try to design for the energy saving target. It is known from Eq. (2), a torque $\mathbf{C_s}$ supplied by the passive compensator is dependent on the item **G**. In an ideal situation under Eq. (2), actuators provide the torque $\mathbf{C_a}$ for dynamic performances of the robot, while the static component **G** is compensated by the balancing device.

From an energy exchange point of view, in an unbalanced robot, an actuation system must provide the energy required to shift from one level of gravitational potential energy, E_g, to another according to robotic positions. Once equipped with a balancing mechanism, a balanced robot can transfer energy during motion. Specifically, Figure 1 shows the detail. Take an articulated robot with two degrees of freedom as an example. When θ_1 (or θ_2) decreases, the gravitational potential energy E_g is transferred from the robot into the balancing mechanism, where it is stored as E_e elastic potential energy and vice versa. The target is to design a device that is able to obtain or give energy according to this way. In this way the global energy required from an actuation system in order to perform a specific task can be significantly reduced.

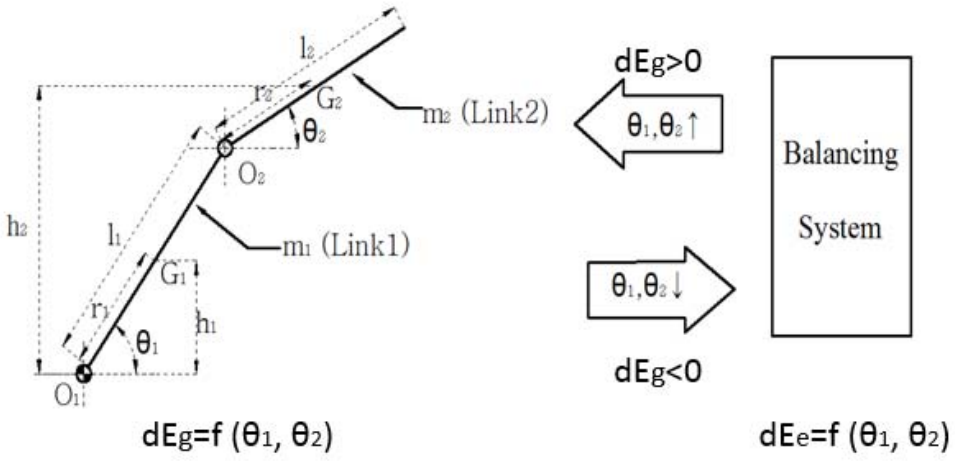

Figure 1. Energy transfer between the robot and the balancing mechanism

2.2 Design steps

Based on the dynamics, a balancing system can be designed from two aspects. The first aspect is the choice for the balancer position. Firstly, we propose a direct way to balance the gravity effect of the robot and satisfy the dynamic requirement. Then, considering practical applications, the balancer proposed should be moved and improved to clear the ambient for the robotic motion. The second aspect is to study the torque from the balancer proposed in the first aspect. To realize perfect balance, the spring parameters are designed to make the spring produce the proper torque to compensate the gravity effect of the robot. With the combination of the two aspects, the perfect balance can be realized.

3. Examples

This section presents two variants of a robot with 2 DOF as examples. The two structures are the study objects needed to be equipped with proper balancing systems. In the first structure (Figure 2), motors M1 and M2 are placed on the ground and the parallelogram linkages are to transfer the motion for the link 2. Compared with Link 1 and Link 2, the masses of Link 3 and Link 4 are negligible. Figure 3 shows another structure with the second motor M2 mounted on the second joint O_2.

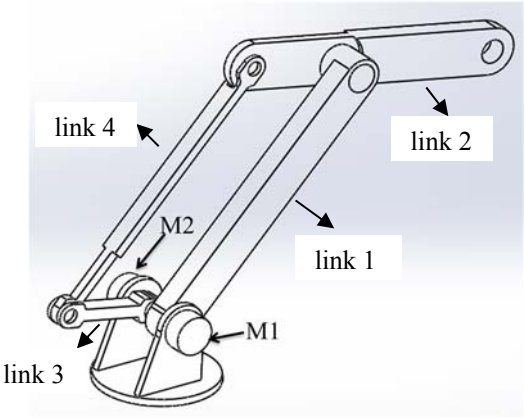

Figure 2. the robotic structure I

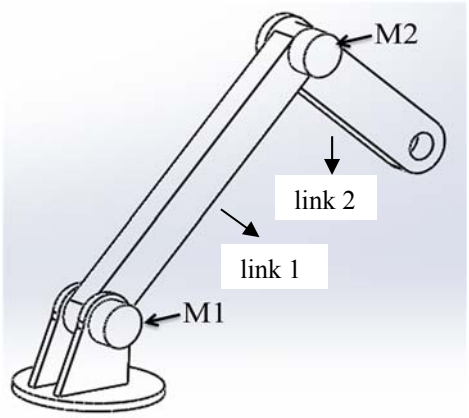

Figure 3. the robotic structure II

In both structures, the masses of Link 1 and Link 2 are only considered. This paper designs balancing systems for both structures. The potential energy for both structures can be expressed in the same way (Figure 1):

$$E_g = m_1 g h_1 + m_2 g h_2 = m_1 g(r_1 \sin\theta_1) + m_2 g(r_2 \sin\theta_2 + l_1 \sin\theta_1). \quad (3)$$

Therefore,

$$\frac{dE_g}{d\theta_1} = m_1 g r_1 \cos\theta_1 + m_2 g l_1 \cos\theta_1, \qquad \frac{dE_g}{d\theta_2} = m_2 g r_2 \cos\theta_2. \quad (4)$$

$$dE_g = \frac{dE_g}{d\theta_1}\cdot d\theta_1 + \frac{dE_g}{d\theta_2}\cdot d\theta_2 = (m_1 g r_1 \cos\theta_1 + m_2 g l_1 \cos\theta_1)\cdot d\theta_1 + (m_2 g r_2 \cos\theta_2)\cdot d\theta_2. \quad (5)$$

In the following sections, balancing systems are designed to balance the torques caused by the two components of Eq. (5)

3.1. Design of a balancer for the robotic structure I

In this section, we propose a balancing system for the first structure from two aspects, based on the robotic dynamics in Section 2. After perfect torque balance is realized, numerical examples verify the conclusion [26].

3.1.1 Evolution of a balancing structure for the structure I

Firstly, we propose a direct way to balance the gravity effect of the robot and satisfy the dynamic requirement, as shown in Figure 4 and Figure 5. Two springs are applied to balance the first and the second links respectively. From Eq. (4), the gravity-effect component of the robot described by θ_1 is $(m_1r_1+m_2l_1)g*\cos\theta_1$, and the component described by θ_2 is $m_2gr_2*\cos\theta_2$. Figure 5 shows a solution. The compensating torque from the first spring is $F_1b_1\cos\theta_1$ and the torque from the second spring is $F_2b_2\cos\theta_2$. Both torques are described by robotic positions (θ_1 and θ_2), therefore they have a close connection with the gravity effect of the robot. To balance the gravity effect, springs should produce constant forces. This requirement can be approximated by means of low stiffness mechanical spring or by means of pneumatic spring connected to big auxiliary volume. In detail, passive compensators are expected to balance the gravity effect of the robot in a perfect way which means the compensating torques exactly counteract the gravity torques and actuators do not need power to contribute the gravity effect. The perfect balance can be realized if,

$$\begin{cases} F_1 b_1 \cos\theta_1 = (m_1 r_1 + m_2 l_1) g \cos\theta_1 \\ F_2 b_2 \cos\theta_2 = m_2 g r_2 \cos\theta_2 \end{cases} \quad (6)$$

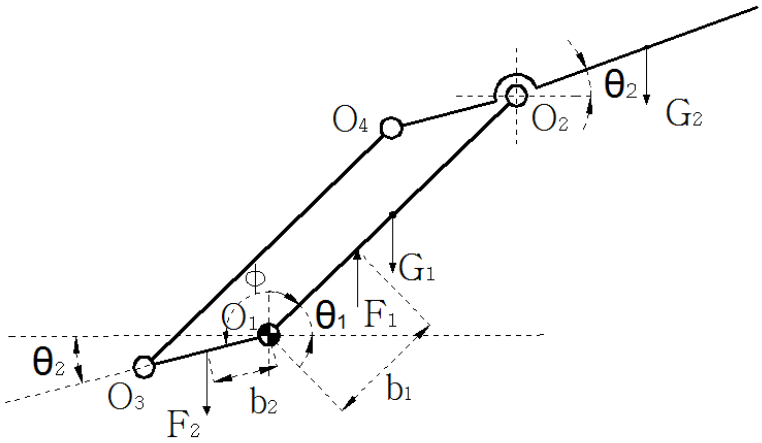

Figure 4. The design of the balancing system

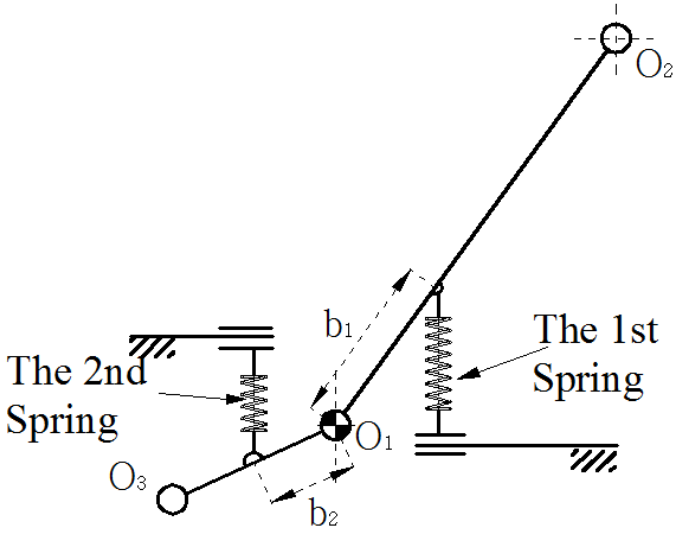

Figure 5. The spring positions

From Figure 5, it is clear that the existence of spring devices can reduce the robot workspace. To release more space, it is better to move the balancing system in other areas that are not used during the robot motion. Figure 6 presents a solution to move the first spring by using a shift angle δ_1. The choice of the angle δ_1 is arbitrary and can be defined considering different requirements that come from specific applications of the robot. A prismatic guide is placed parallel to a new datum line O_1-P_1 for θ_1 so that the 1st spring is perpendicular to the line O_1-P_1, therefore the spring produces a spring torque $F_1 b_1 \cos\theta_1$. Using this way, whatever a value of δ_1, a proper position can be always found for the 1st spring to produce a spring torque $F_1 b_1 \cos\theta_1$ decided by the angle θ_1. With this skill, we can decide δ_1 and the length of the connecting link b_1 so that the spring is placed at a proper position. The second spring can also be placed at a proper position using the same approach (Figure 7). Here, we choose $\delta_1 = \pi/2$, $\delta_2 = \pi/2$ to place the two springs, shown in Figure 8.

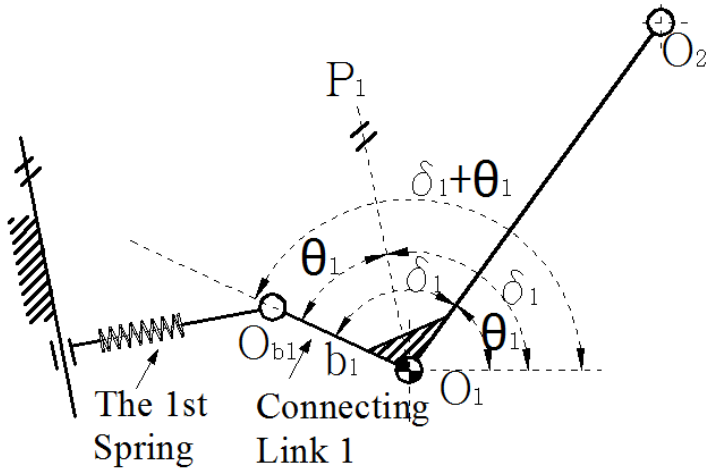

Figure 6. A solution to place the 1st spring

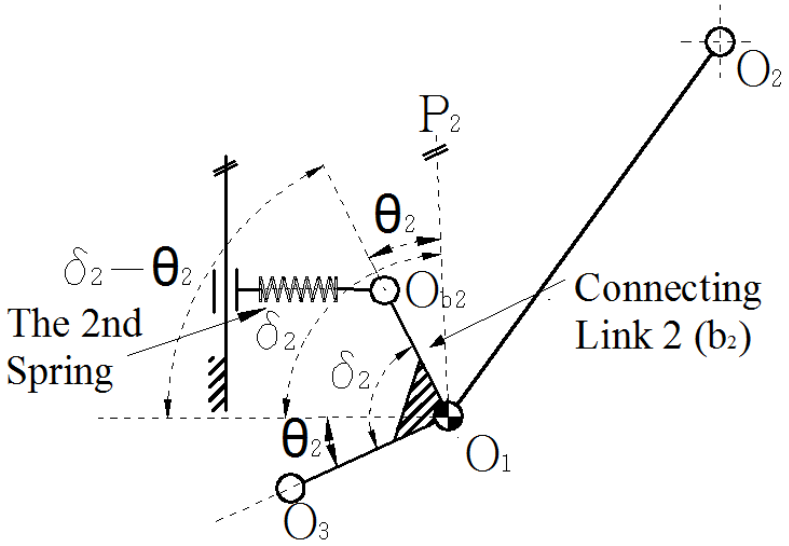

Figure 7. A solution to place the 2nd spring

Since the prismatic guides normally require much space for placing the guides, they are substituted with revolute joints, as shown in Figure 9. With the substitution, torque errors happen since with revolute joints, a torque produced by a spring is not always $F_1 b_1 \cos\theta_1$ (or $F_2 b_2 \cos\theta_2$). During the robotic motion, the springs rotate and the torques are decided not only by robotic positions, but also by relative positions of the springs with respect to the robot. In the following part, we will discuss how to find the best position for the fixed pivot O_5 (or O_6) so that the error between the torque caused by the 1st (or 2nd) spring and the gravity torque of Link 1 (or Link 2) is as little as possible. Also, spring parameters are studied to decrease or eliminate the error. It is perfectly static balancing if the torques from the springs can compensate the gravity torque of the robot in every configuration.

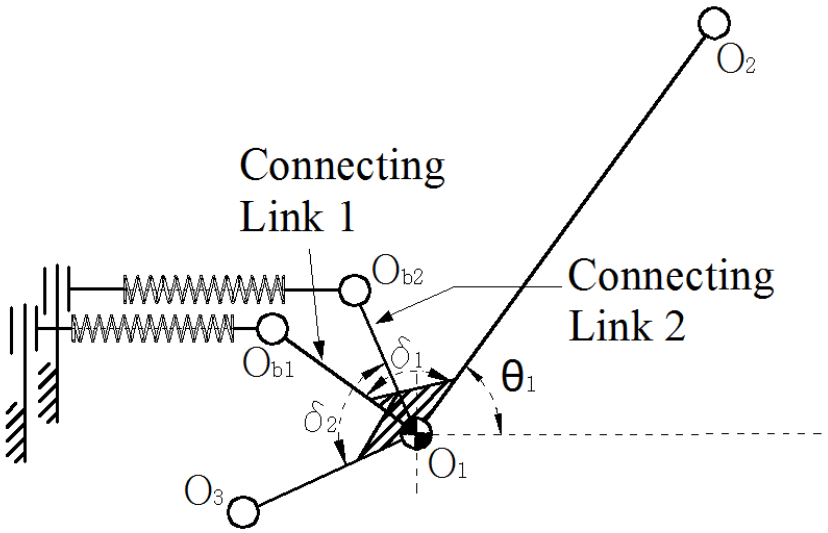

Figure 8. The Placement of the two springs

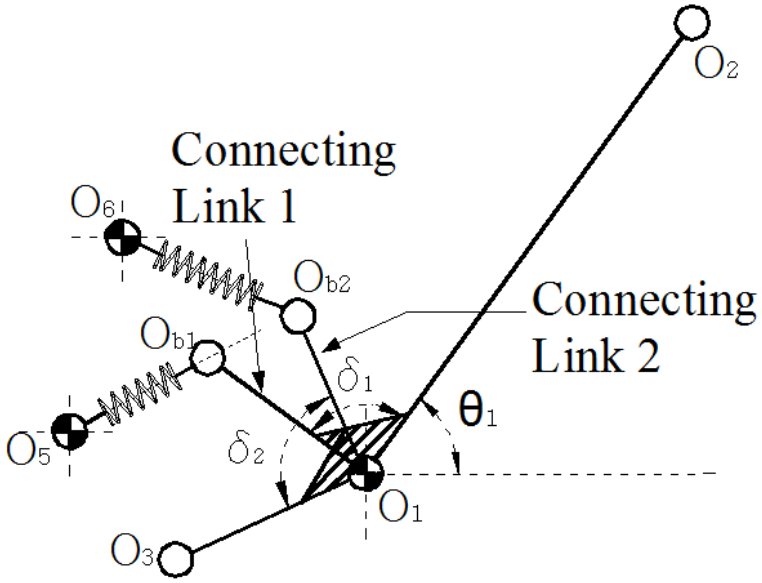

Figure 9. A feasible design using revolute joints

3.1.2. Analysis of torque compensation and design of spring parameters

In this part, spring torques are analyzed with the choice of spring parameters. We start the design of a balancing device from Link 1. In Figure 10, the position of the fixed pivot O_5 can be described with r_5 and α_5 in polar coordinate. A spring is possibly designed in two ways (Figure 10 (a) and (b)), depending on spring force and space dimensions. In the first way, a spring is connected by two articulated joints O_5 and O_{b1}. In the second way, a spring is guided to avoid the separation of the spring and the link articulated with the joint O_5. In following research, the second design is taken as an example. In the triangle $\Delta O_1O_{b1}O_5$, the varied length of the 1st spring a_1 is expressed:

$$a_1 = a_1(\theta_1) = \sqrt{r_5^2 + b_1^2 - 2b_1 r_5 \cos(\alpha_5 - \theta_1)}\,, \qquad a_1 \sin\mu_1 = b_1 \sin(\alpha_5 - \theta_1) \tag{7}$$

The moment arm of the 1st spring is:

$$b_{1F} = r_5 \sin \mu_1 \tag{8}$$

So the torque applied by the balancing system is:

$$C_{1F}(\theta_1) = F_{1F} \cdot b_{1F} \tag{9}$$

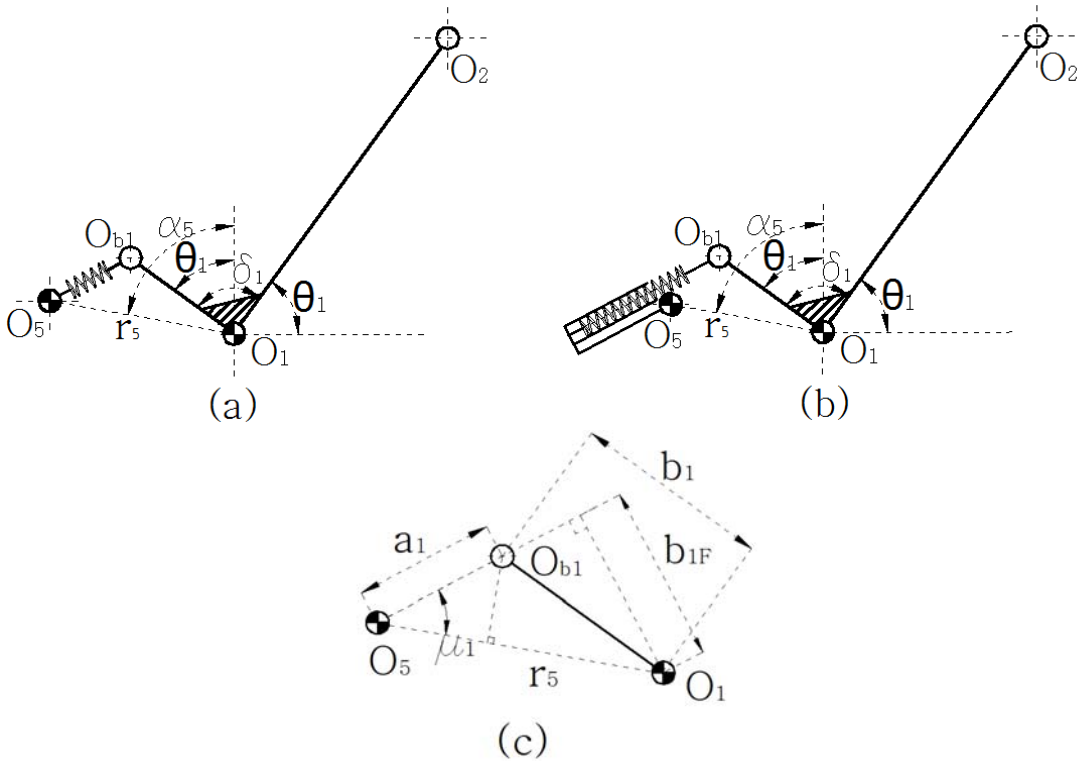

Figure 10. Design of a balancing device for Link 1

Here, we classify the force F_{1F} applied by the spring into two cases: (i) constant force and (ii) variable force. Both cases can be realized in reality, using different devices.

(i) Constant force.

Assume that F_{1F} is the constant force which value equals the one when the maximum torque from Link 1 is compensated. It is known, from Eq. (6), that:

$$C_{1max} = C_1(\theta_1 = 0) = (m_1 r_1 + m_2 l_1)g\,, \qquad F_{1F} \cdot b_{1F(\theta_1=0)} = C_{1max} \tag{10}$$

Therefore,

$$F_{1F} = \frac{C_{1max}}{b_{1F(\theta_1=0)}} \tag{11}$$

The error needed to be compensated by an actuator is,

$$e_c = C_1(\theta_1) - C_{1F}(\theta_1) \tag{12}$$

The target is to reduce the error as much as possible. From Eq. (12), the error depends on the angle θ_1: different angles imply different errors and different positions of Link 1.

(ii) Variable force.

In this case, we set the force F_{1FK} on the spring is variable, which value depends on the spring deformation. It is known that,

$$F_{1FK} = F_{1F0} + k_{1id} \cdot \Delta a_1 \tag{13}$$

Where $\Delta a_1 = a_1 - a_{10}$, a_{10} is the spring deformation when F_{1FO} is loaded and θ_1 is zero. Then the balancing torque is:

$$\begin{aligned} C_{1FK} &= F_{1FK} \cdot b_{1F} = (F_{1F0} + k_{1id} \cdot \Delta a_1) \cdot b_{1F} \\ &= [F_{1F0} + k_{1id} \cdot (a_1 - a_{10})] \cdot \frac{r_5 \cdot b_1}{a_1} \sin(\alpha_5 - \theta_1) \end{aligned} \tag{14}$$

Especially, if $\alpha_5 = \pi/2$, considering Equations (7), (8), Equation (14) can be evolved as:

$$\begin{aligned} C_{1FK} &= F_{1FK} \cdot b_{1F} \\ &= F_{1F0} \cdot \frac{r_5 \cdot b_1}{a_1} \cdot \cos\theta_1 + k_{1id} a_1 \cdot \frac{r_5 \cdot b_1}{a_1} \cdot \cos\theta_1 - k_{1id} a_{10} \cdot \frac{r_5 \cdot b_1}{a_1} \cdot \cos\theta_1 \\ &= (F_{1F0} - k_{1id} a_{10}) \cdot \frac{r_5 \cdot b_1}{a_1} \cdot \cos\theta_1 + k_{1id} r_5 b_1 \cdot \cos\theta_1 \end{aligned} \tag{15}$$

The value of the balancing torque must be equal to the value of the torque from the link, then a perfect balancing can be realized, as shown in the equation (16):

$$C_{1FK} = C_1 = C_{1max} \cdot \cos\theta_1 \tag{16}$$

In this case, we can obtain the conditions satisfying the equation (16):

$$F_{1F0} = k_{1id} \cdot a_{10} \ , \ \ k_{1id} r_5 b_1 = C_{1max} \tag{17}$$

Therefore, the spring can be deformed by a_{10} to obtain the force F_{1F0}. We have the spring stiffness as:

$$k_{1id} = \frac{C_{1max}}{r_5 b_1} \tag{18}$$

In this way, no error exits and Link 1 can be compensated perfectly.

Now assume an arbitrary spring with the stiffness k_1 applied in the balancing mechanism, the torque error can be defined in percentage as,

$$e_{C\%} = \frac{C_{1FK} - C_1}{C_{1max}} \cdot 100 \tag{19}$$

Considering Eq. (15), Eq. (19) can be evolved as,

$$e_{C\%} = \frac{F_{1F0} \cdot \frac{r_5 \cdot b_1}{a_{10}} \left(\frac{a_{10}}{a_1} - \frac{k_1 a_{10}^2}{F_{1F0} \cdot a_1} + \frac{k_1 a_{10}}{F_{1F0}}\right) \cdot \cos\theta_1 - C_{1max} \cdot \cos\theta_1}{C_{1max}} \cdot 100$$
$$= \left[\left(\frac{a_{10}}{a_1} - \frac{k_1 a_{10}^2}{F_{1F0} \cdot a_1} + \frac{k_1 a_{10}}{F_{1F0}}\right) - 1\right] \cdot \cos\theta_1 \cdot 100 \quad (20)$$

It is known from Eq. (17), the ideal spring must have a deformation a_{10} to obtain the proper force F_{1F0} for the torque compensation of the manipulator.

Since a_{10} is the distance between the connection points of the spring, when $\theta_1 = 0$. This means that the spring must have an initial length of the same order of a_{10} and this means also that the encumbrance of the spring can lead to practical installation problems (like in fig. 10 b). To solve this problem, a spring with a bigger value of the stiffness can produce the required force in the initial condition ($\theta_1 = 0$) with shorter deformation but it will have the error in torque in the other positions. The following analysis is done to evaluate this error. For example, if we have:

$$k_1 = n \cdot k_{1id} = n \cdot \frac{F_{1F0}}{a_{10}} \quad (21)$$

Here n is the stiffness ratio between the actual spring and the ideal spring. In this case, the deformation is shortened as 1/n of the previous one. Then the Eq. (20) is evolved as,

$$e_{C\%} = \left(\frac{a_{10}}{a_1} - n\frac{a_{10}}{a_1} + n - 1\right) \cdot \cos\theta_1 \cdot 100 \quad (22)$$

Considering Eq. (7), if we introduce the ratio $ra_1 = r_5/b_1$ to have a non-dimensional evaluation, Eq.(22) is evolved as,

$$e_{C\%} = \left(\frac{\sqrt{1+ra_1^2}}{\sqrt{1+ra_1^2 - 2 \cdot ra_1 \sin\theta_1}} - n \cdot \frac{\sqrt{1+ra_1^2}}{\sqrt{1+ra_1^2 - 2 \cdot ra_1 \sin\theta_1}} + n - 1\right) \cdot \cos\theta_1 \cdot 100 \quad (23)$$

Figure 11 shows that when the balancer is located at $\alpha_5=\pi/2$, the error $e_{C\%}$ changes as the spring stiffness varies. It means that a designer can choose the proper stiffness with the matched deformation according to different practical requirements. If n=1 eq. 23 represents the ideal case of perfect balance and $e_{C\%}$ is equal to zero. It is realized that even if n = 2, the stiffness k_1 is twice than the ideal stiffness k_{1id}, the error is no more than around 15%. We can also observe that the error figure is not globally symmetric within the range (0, 2π), but local symmetric within areas (0, π) and (0, $-\pi$). After we take the absolute value of $e_{C\%}$, the error is then evaluated in a mean value way $e_{C\%mean}$, as shown in Figure 12.

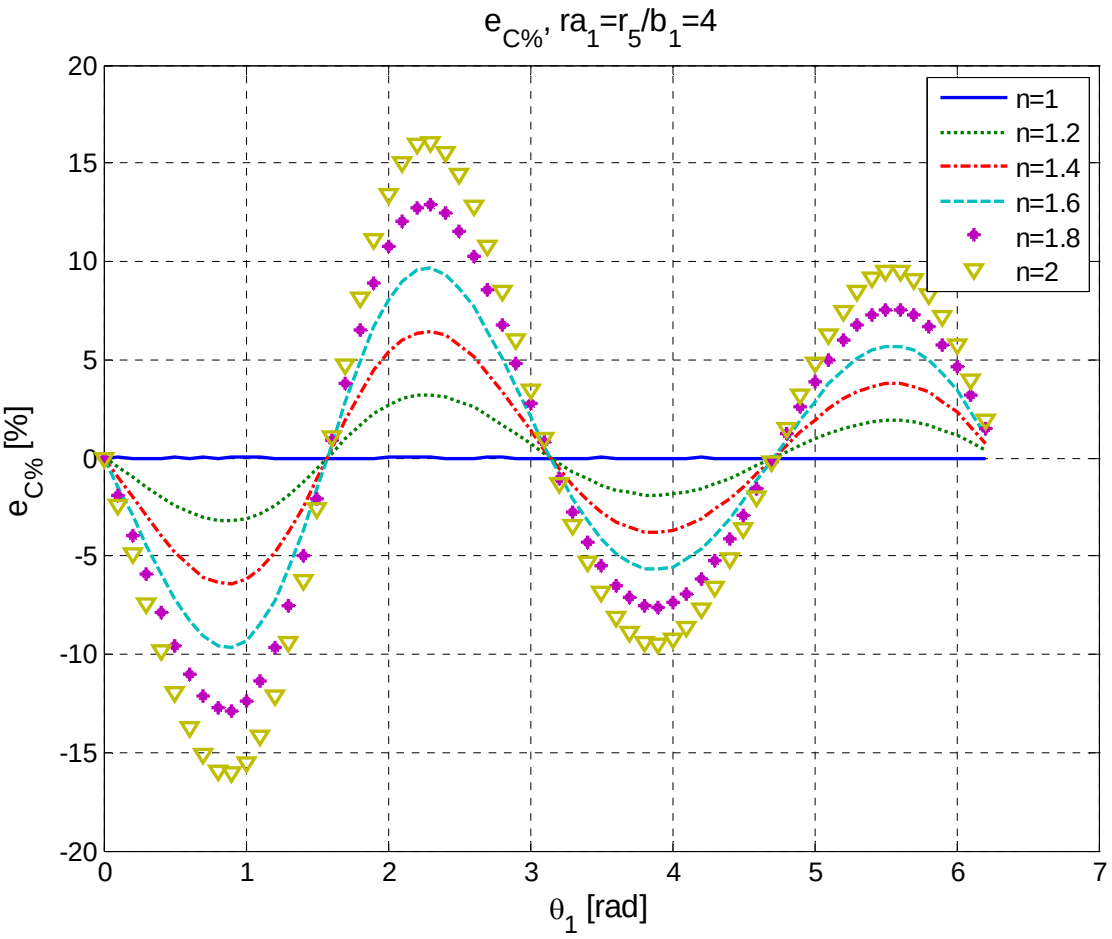

Figure 11. The error between the 1st spring torque and the torque from the Link 1 when $ra_1=4$ and the spring stiffness is varying.

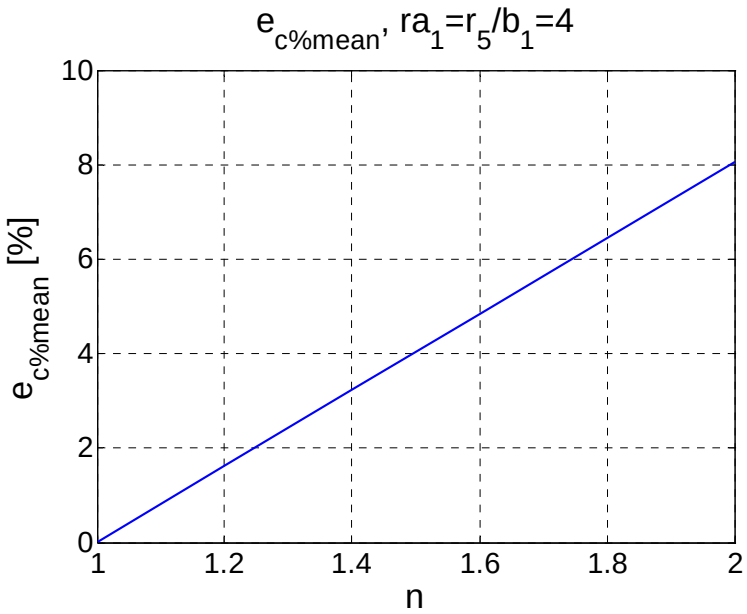

Figure 12. The error between the 1st spring torque and the torque from the Link 1 in the mean value.

Next, we discuss how to realize the static balancing for Link 2 in a feasible way. The process is the same as before if we change subscript '1' with '2' for the Link 2. In Figure 13, the position of the

fixed pivot O_6 is described with r_6 and α_6 in polar coordinate. Also the maximum torque is,

$$C_{2max} = C_2(\theta_2 = 0) = m_2 r_2 g \tag{24}$$

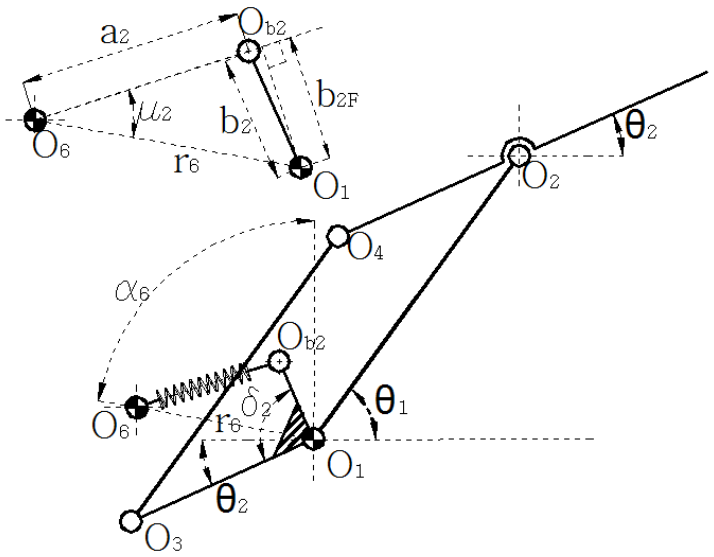

Figure 13. Design of a balancing device for Link 2

3.1.3. Numerical examples

This part shows numerical examples to test and verify the balancing effect of the balancer mentioned above. Weight and dimensions are listed in Table 1.

Table 1. Robot physical parameters

physical parameters	m_1	m_2	l_1	l_2	r_1	r_2	b_1	b_2
values	100	40	1.2	1	0.6	0.5	0.2	0.2

(i) Constant force for Link 1.

For the 1st link, when the spring provides with a constant force and the range of θ_1 is $(-\pi/2, \pi/2)$. Figure 14 shows the spring torque C_{1F}, compared with the gravity torque C_1 as a function of θ_1 in a constant-force case, when α_5 is different and $ra_1 = r_5/b_1 = 6$. ra_1 is used to describe the non-dimensional position for the pivot O_5. Every smooth curve means the spring torque at every position described by α_5 and ra_1. The dotted curve means the gravity torque. From the figure, for the curve $\alpha_5 = 84^\circ$, for example, the spring torque is firstly bigger than the gravity torque and the error is therefore positive. Then, as θ_1 increases, the curve gets closer to the gravity torque and finally less than the gravity torque with the error becoming negative. We can observe the curve with $\alpha_5=86^\circ$ is the best result among the batch of curves: this curve goes along the dotted curve, which means the torque supplied by the spring almost compensates the gravity torque. Here only torque changes at $ra_1 = 6$ are shown in this paper. In Figure 15, conclusions about different ra_1 are shown. A bigger value of ra_1 shows little error between the spring torque and the gravity torque. It is not difficult to know that with a bigger value of ra_1, the error becomes little, because the bigger value of ra_1 implies the position of the fixed pivot O_5 goes further away from the point O_1. At an infinite position, the revolute joint will ideally evolve into a prismatic guide and there is no error for a prismatic pair. It is known from Figure 15, when $\alpha_5=86^\circ$ and $ra_1=r_5/b_1=6$, the least error is obtained as about 2.8%.

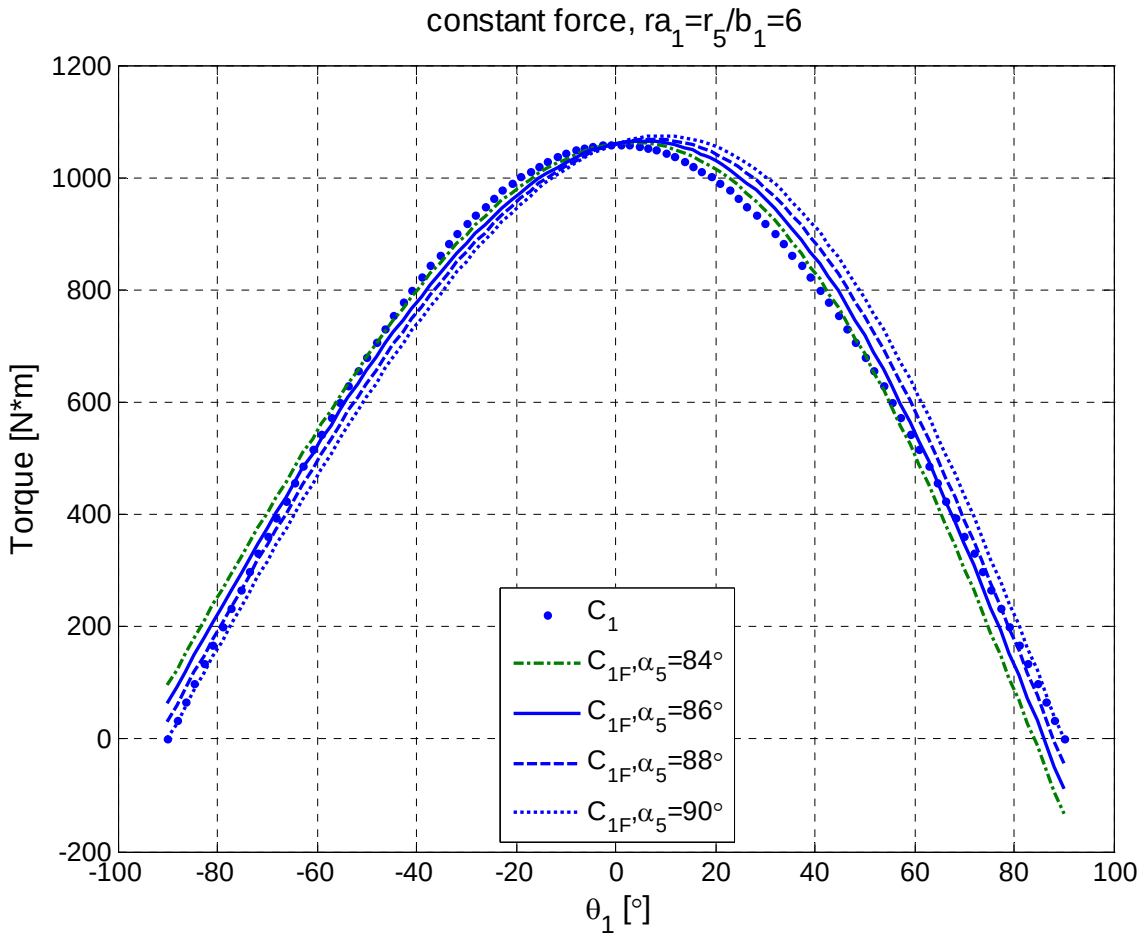

Figure 14. The 1st spring torque and the torque from the Link 1 in a constant-force case.

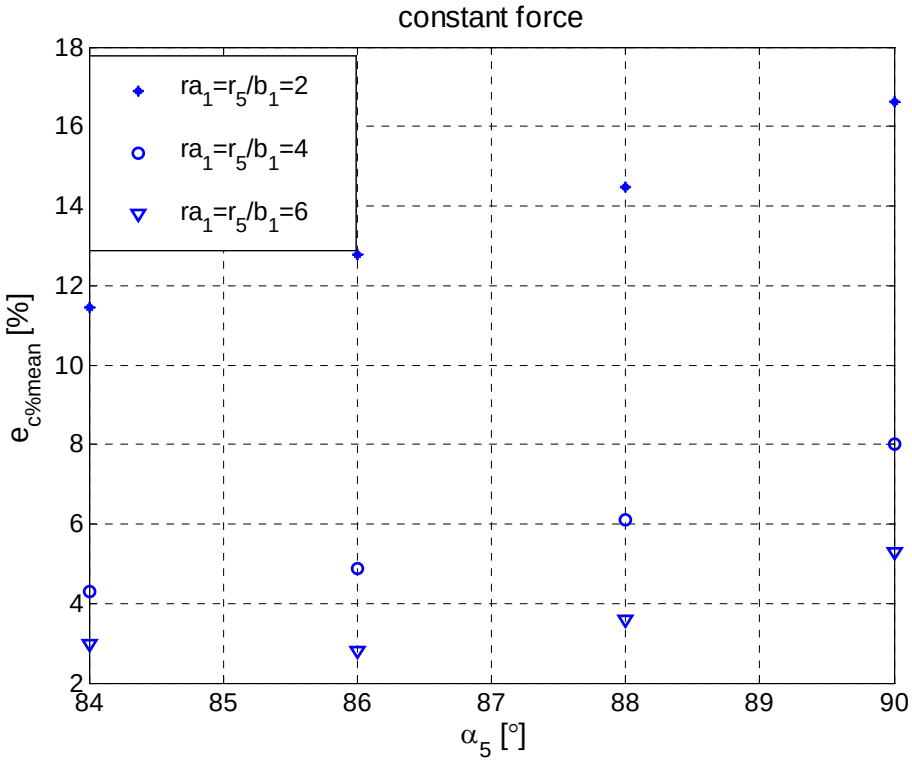

Figure 15. The error between the 1st spring torque and the torque from the Link 1 in a constant-

force case.

(ii) Variable force for Link 1.

Figure 16 shows the 1st spring torque, compared with the gravity torque described by θ_1 in a variable-force case. The spring stiffness, the initial length and the initial force are decided by the requirements of the torque compensation discussed in Section 3.1.2. The perfect balance is realized at $\alpha_5=90°$ where Figure 17 shows the error is zero. Also, the ratio ra_1 has no influence on the error, which means, when a spring produces a variable force with ideal parameters defined in the equations (17), (18), the error is only dependent on the orientation of the spring, not on the distance away from the point O_1.

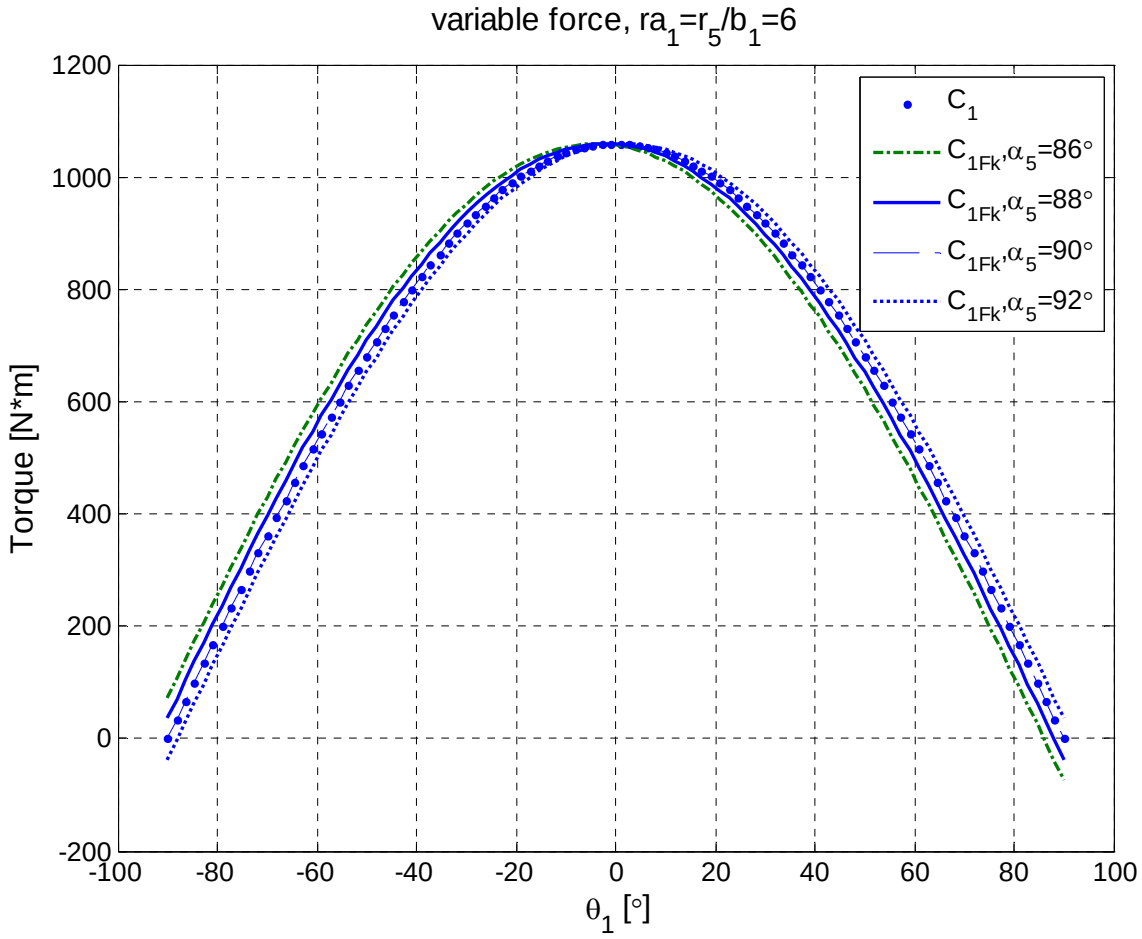

Figure 16. The 1st spring torque and the torque from the Link 1 in a variable-force case.

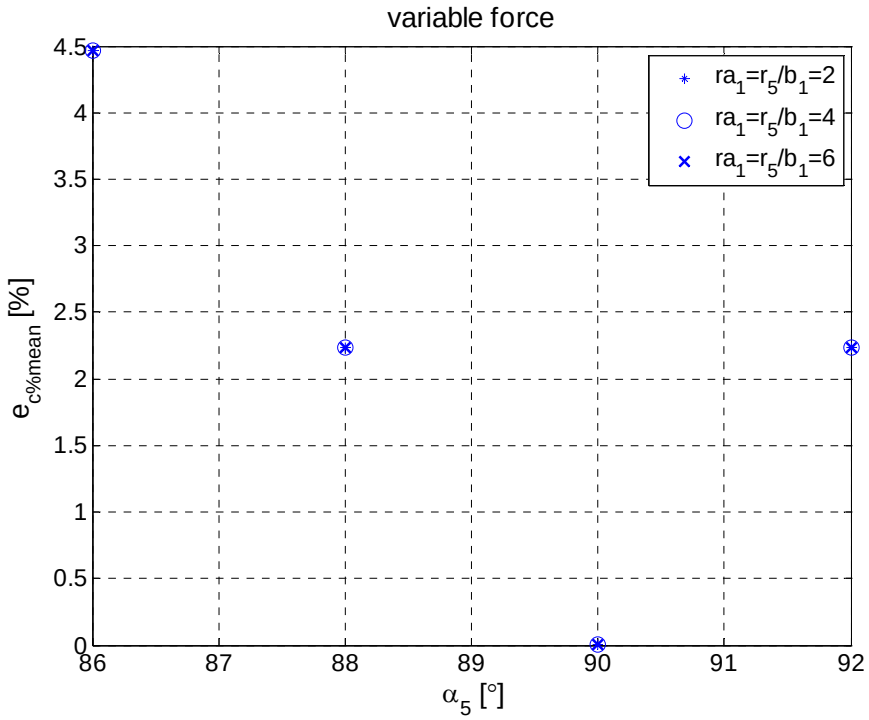

Figure 17. The error between the 1st spring torque and the torque from the Link 1 in a variable-force case.

(iii) Constant force for Link 2.

For the study of the 2nd link, it is known that the gravity torque is influenced by the position of the 1st link. So if we assume the range of θ_2 is controlled by θ_1 and ϕ (Figure 4), θ_2 can be known from the relation: $\theta_2 = \phi+\theta_1-\pi$. The choice of ϕ should consider the singularity problem. When ϕ equals 0 or π, the singularity is happened. Here, ϕ varies from 18° to 162° as an example. Figure 18 shows a batch of curves in a constant-force situation in the conditions $ra_2 = r_6/b_2 = 6$, $\alpha_6 = 92°$. When the θ_1 is fixed and ϕ changes, θ_2 is therefore changed. During the change of θ_2, the spring torques and the required balancing torque are drawn as smooth and dotted curves respectively. Then with other values of θ_1, we follow the same way to define θ_2 and produce torque changes. Figure 19 shows, among different positions of the joint pivot O_6 described by α_6 and ra_2, the optimization result for the error is least as about 5%, when $\alpha_6 = 90°$ and $ra_2 = 6$.

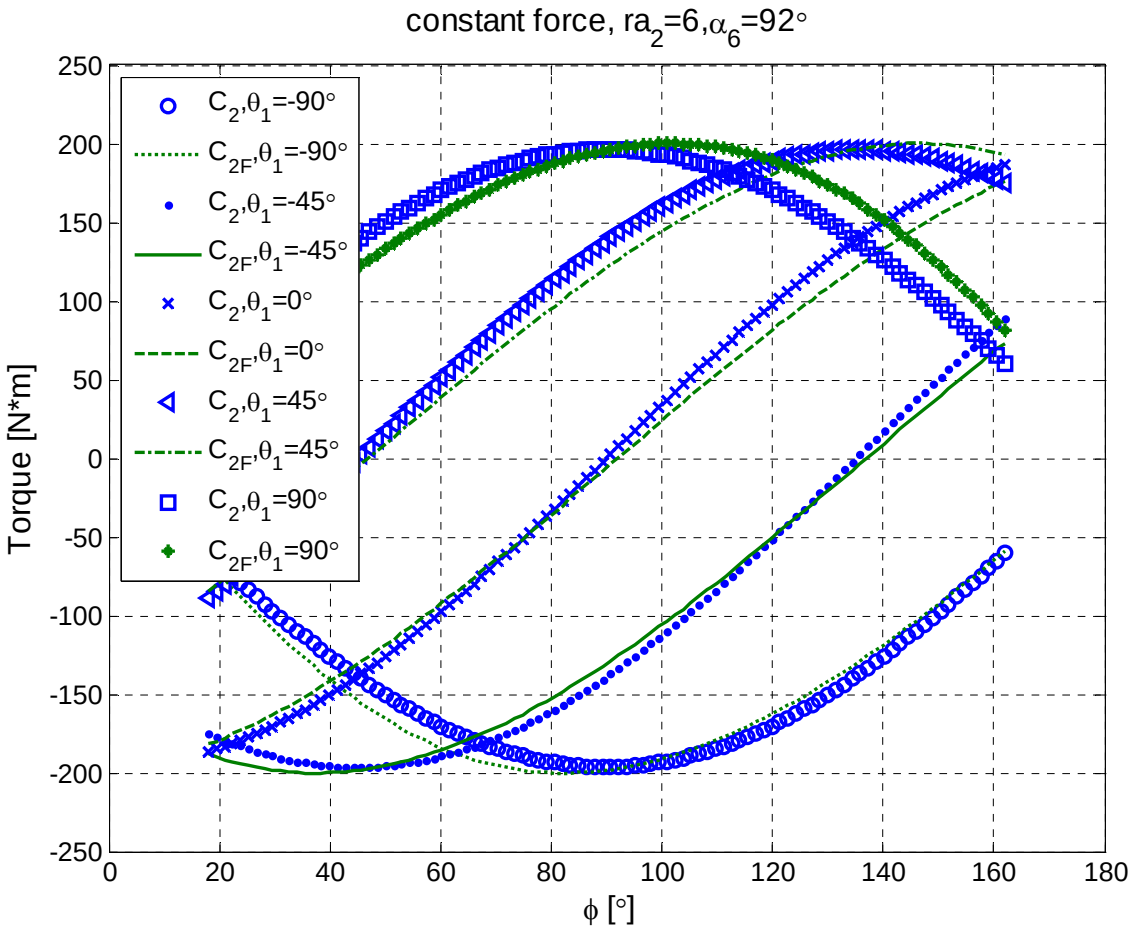

Figure 18. The 2nd spring torque and the torque from the Link 2 in a constant-force case.

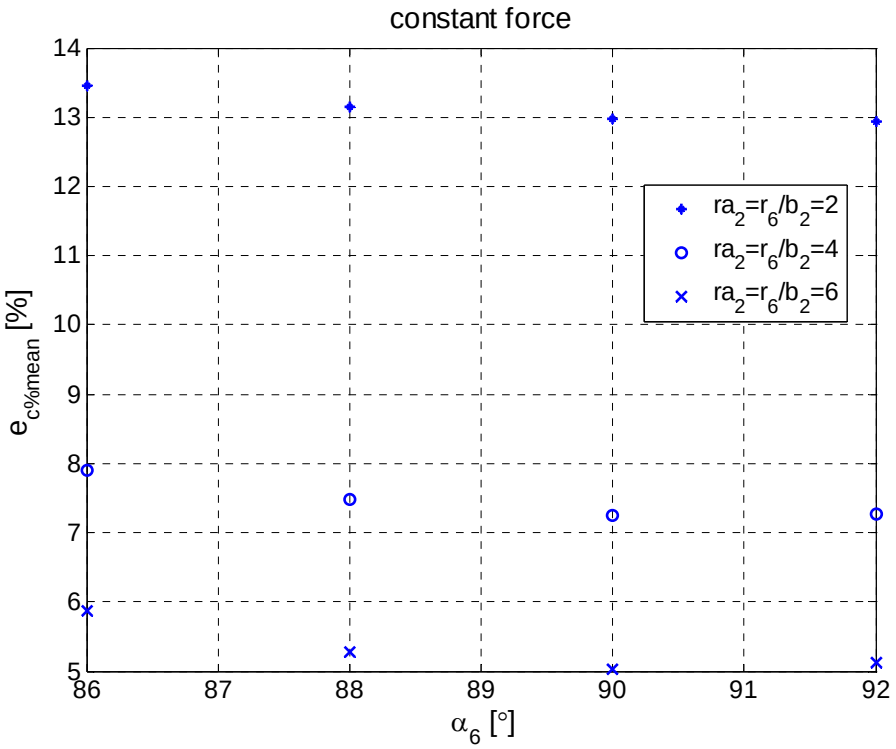

Figure 19. The error between the 2nd spring torque and the torque from the Link 2 in a constant-force case.

(iv) Variable force for Link 2.

Figure 20 shows the 2nd spring torque, designed according to ideal parameters of eq. 17 but referred to the second link, compared with the gravity torque from Link 2 in a variable-force case, when α_6=92°. Figure 21 shows the error $e_{C\%mean}$ as a function of α_6, and it is zero when α_6=90°. Also, the error has no relation with the value of the ratio ra_2.

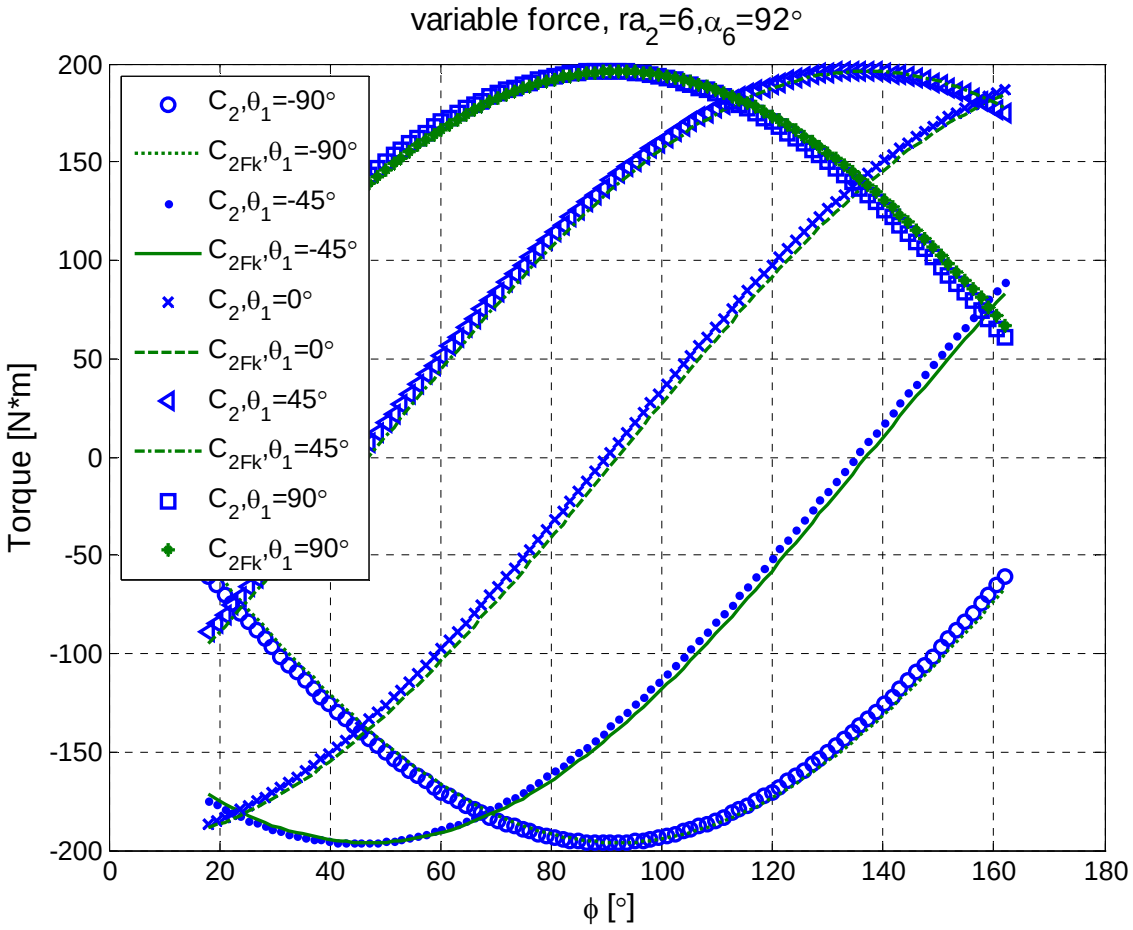

Figure 20. The 2nd spring torque and the torque from the Link 2 in a variable-force case.

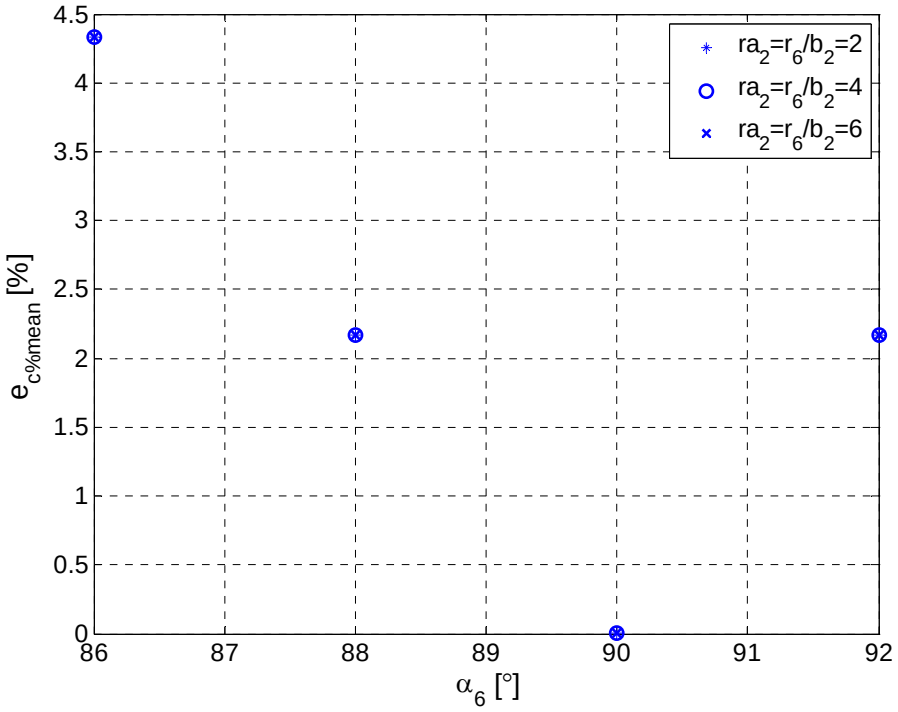

Figure 21. The error between the 2nd spring torque and the torque from the Link 2 in a variable-force case.

3.2. Design of a balancer for the robotic structure II

This part focuses on the design of the balancing system for the robotic structure II, as shown in Figure 3. The balancing system consists of cable, pulleys, cross mechanisms and springs [27]. The two design aspects, the position of the balancer and the design of spring parameters, are discussed. For spring choice, pneumatic and hydro-pneumatic springs are studied.

3.2.1 Evolution of a balancing structure for the structure II

Consider the first link as a 1 DOF situation without the connection of Link 2. The balancing device consists of the cross mechanism and the spring. Figure 22 shows two possibilities to place a balancing device. The position of the balancing device can be decided by δ_1 and b_1, considering free volume around the robot. With a cross mechanism, rotational movement is transferred into translational one. F_1 is a constant force applied by the spring, which can be realized by a pneumatic spring introduced later. M_1 is Motor 1 driving the first link.

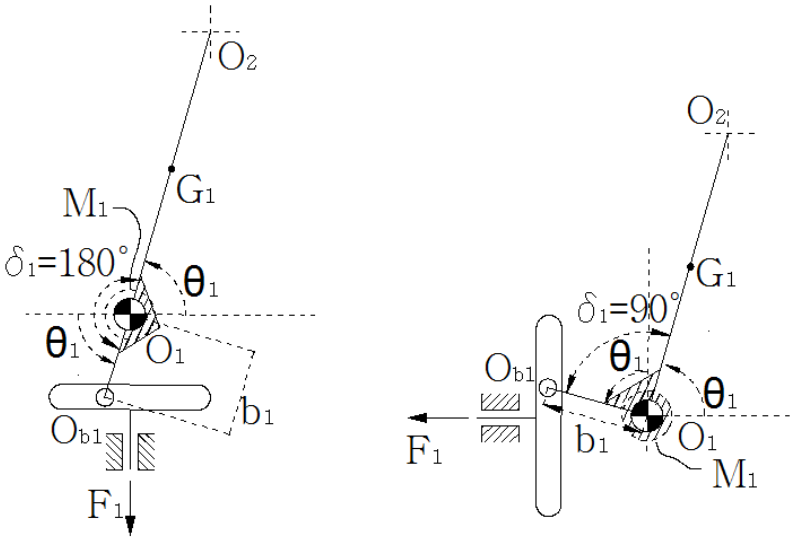

Figure 22. A balancing device for the first link.

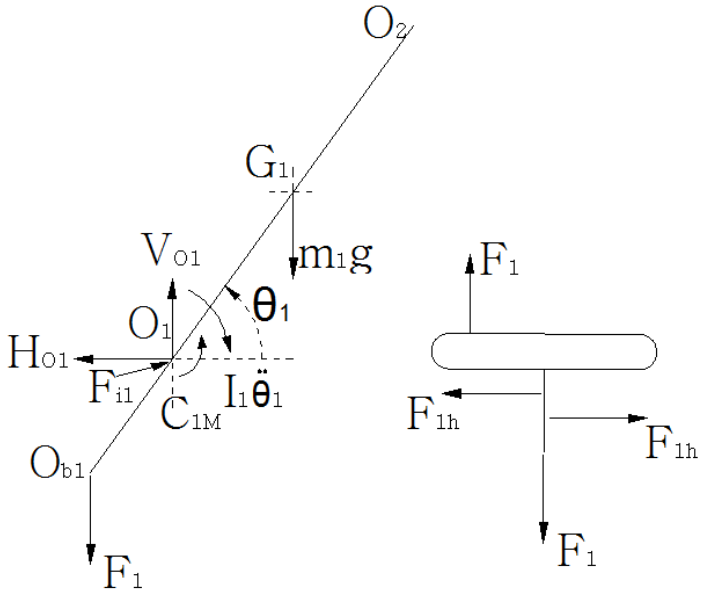

Figure 23. Free body diagram for Link 1 and the cross mechanism in 1 DOF situation.

Take the left part of Figure 22 as an example. From its free body diagram (Figure 23), it is known the dynamic description of Link 1 is

$$F_1 b_1 \cos\theta_1 + C_{1M} = m_1 g r_1 \cos\theta_1 + I_1 \ddot{\theta}_1. \tag{25}$$

Under the perfectly static balancing situation $\ddot{\theta}_1 = 0$, the torque provided by the motor M_1 must be null, i.e. $C_{1M} = 0$, then,

$$F_1 b_1 \cos\theta_1 = m_1 g r_1 \cos\theta_1. \tag{26}$$

If we assume that,

$$F_1 b_1 \cos\theta_1 = \frac{dE_e}{d\theta_1}, \qquad m_1 g r_1 \cos\theta_1 = \frac{dE_g}{d\theta_1}. \tag{27}$$

Then we have,

$$\frac{dE_e}{d\theta_1}d\theta_1 = \frac{dE_g}{d\theta_1}d\theta_1. \tag{28}$$

Compared with Eq. (5), an ideal balancing device is realized if we develop a system that is able to produce a constant force and to obtain or provide energy according to Eq. 27.

Figure 24 shows the synthesis of the balancing devices for Link 1 and Link 2. The motor M_1 provides a torque C_{1M} between the frame and Link 1, motor M_2 provides a torque C_{2M} between the links 1 and 2. Considering Link 1 as a part of the robot (Figure 25 and Figure 26), it is known,

$$\begin{aligned} &F_1 b_1 \cos\theta_1 + C_{1M} - C_{2M} - m_2 r_2 l_1 \sin(\theta_1 - \theta_2)\dot{\theta}_2^2 - m_2 r_2 l_1 \cos(\theta_1 - \theta_2)\ddot{\theta}_2 = \\ &= (m_1 r_1 + m_2 l_1) g \cos\theta_1 + (I_1 + m_2 l_1^2)\ddot{\theta}_1. \end{aligned} \tag{29}$$

Under perfectly static balancing situation $\dot{\theta}_2 = 0$ and $\ddot{\theta}_1 = \ddot{\theta}_2 = 0$, the torques provided by the motors M_1 and M_2 must be null, i.e. $C_{1M} = C_{2M} = 0$, then we can have:

$$F_1 b_1 \cos\theta_1 = (m_1 r_1 + m_2 l_1) g \cos\theta_1. \tag{30}$$

$$F_1 b_1 \cos\theta_1 = \frac{dE_e}{d\theta_1}, \qquad (m_1 r_1 + m_2 l_1) g \cos\theta_1 = \frac{dE_g}{d\theta_1}. \tag{31}$$

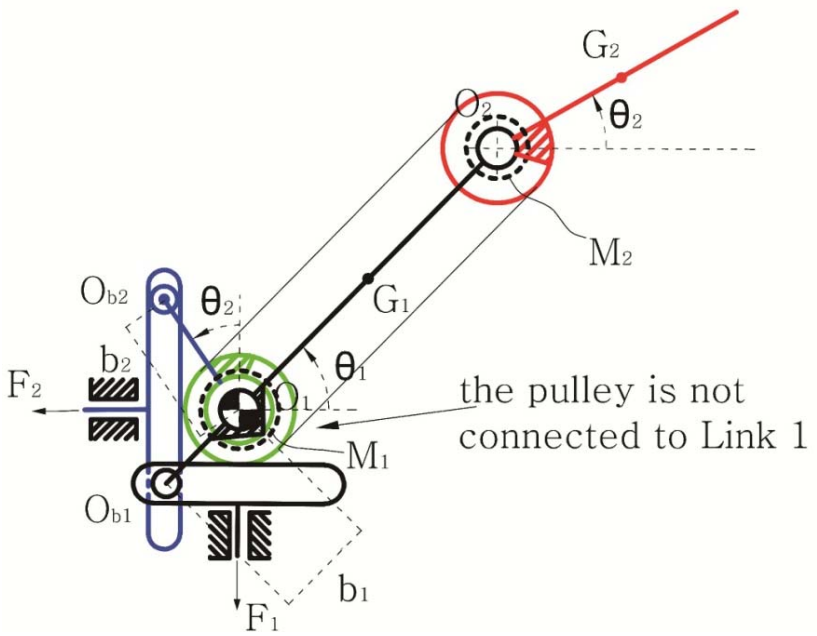

Figure 24. Balancing device for the two DOF robot.

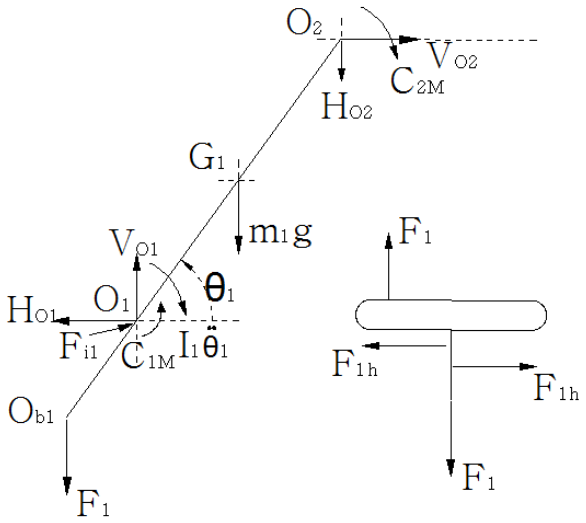

Figure 25. Free body diagram for Link 1 and the cross mechanism in 2 DOF situation.

For Link 2, Figure 24 shows a possibility of the balancing device for the second link. The rotation of the link 2 is transferred by means of the cable-pulleys mechanism to the rotation of the link O_1-O_{b2} that is fixed on the lower pulley. The pulley is not connected to the link 1, but has the same rotational axis as Link 1. F_2 is a constant force applied by a spring device. It is known the dynamic description of Link 2,

$$F_2 b_2 \cos\theta_2 + C_{2M} = m_2 g r_2 \cos\theta_2 + I_2 \ddot{\theta}_2. \tag{32}$$

Under perfectly static balancing situation, $C_{2M} = 0$ and $\ddot{\theta}_2 = 0$, then,

$$F_2 b_2 \cos\theta_2 = m_2 g r_2 \cos\theta_2. \tag{33}$$

If we assume that,

$$F_2 b_2 \cos\theta_2 = \frac{dE_e}{d\theta_2}, \qquad m_2 g r_2 \cos\theta_2 = \frac{dE_g}{d\theta_2}. \tag{34}$$

Then we have,

$$\frac{dE_e}{d\theta_2} d\theta_2 = \frac{dE_g}{d\theta_2} d\theta_2. \tag{35}$$

An ideal balancing device is realized if we develop a system that can work according to Eq. (5). Combining Eq. 5, Eq. 28, and Eq. 31-35, Eq. 36 is evolved. In this way, the energy can be transferred between the robot and the balancing system.

$$dE_g = \frac{dE_g}{d\theta_1}\cdot d\theta_1 + \frac{dE_g}{d\theta_2}\cdot d\theta_2 = \frac{dE_e}{d\theta_1}\cdot d\theta_1 + \frac{dE_e}{d\theta_2}\cdot d\theta_2 = F_1 b_1 \cos\theta_1 d\theta_1 + F_2 b_2 \cos\theta_2 d\theta_2 = dE_e. \tag{36}$$

Also, there is a screw that fixes the link O_1-O_{b2} to the lower pulley. This solution represents the possibility of adjusting the relative position between the lower pulley and the link, which adapts the system to different positions of the center of the gravity for Link 2, due to different types of payloads and an end effector on Link 2, as shown in Figure 27.

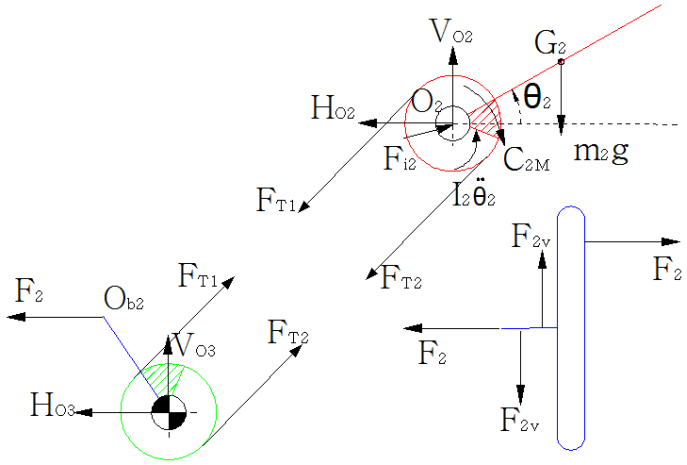

Figure 26. Free body diagram of two pulleys and a cross mechanism.

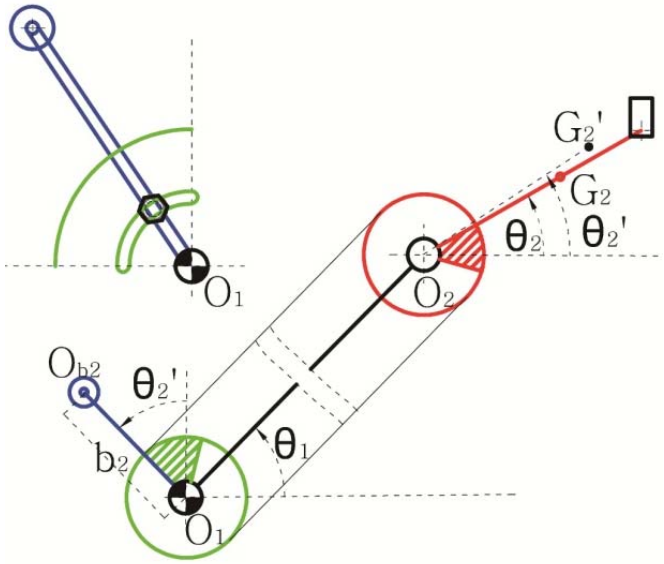

Figure 27. Little adjustment for the new center of gravity.

3.2.2. (Hydro-) Pneumatic spring and design of spring parameters

A mechanical spring can be designed to satisfy force and torque requirements. However a mechanical spring with large dimensions takes much space. A pneumatic or hydro-pneumatic spring with a compact working chamber takes little space and allows much space for the robot. The pneumatic or hydro-pneumatic spring with an auxiliary volume is used to apply almost constant forces.

A pneumatic spring consists of a working chamber and an auxiliary bladder both filled with gas, which works in an adiabatic condition, with negligible friction effects. Figure 28 illustrates its work principle. Assume P_0 and V_0 are the initial pressure and volume in the spring. P_0 can be controlled to make the system produce the constant force required. It is known that in an adiabatic condition,

$$P_1V_1 = P_0V_0, \qquad V_1 = V_{aux} + x_1A_1. \tag{37}$$

Here, assume that the volume of the bladder is much bigger than that of the chamber. So,

$$F_1 = P_1 A_1 = \frac{P_0 V_0}{V_1} A_1 = \frac{P_0 V_0}{V_{aux} + x_1 A_1} A_1 \approx \frac{P_0 V_0}{V_{aux}} A_1 = \text{const.} \tag{38}$$

In this way, the pneumatic spring supplies an approximately constant force to support a manipulator. The bladder can be placed far away from the robot, therefore, the robot can have much space for its tasks.

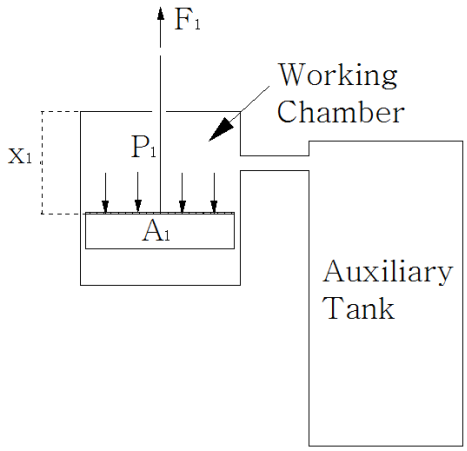

Figure 28. the pneumatic spring

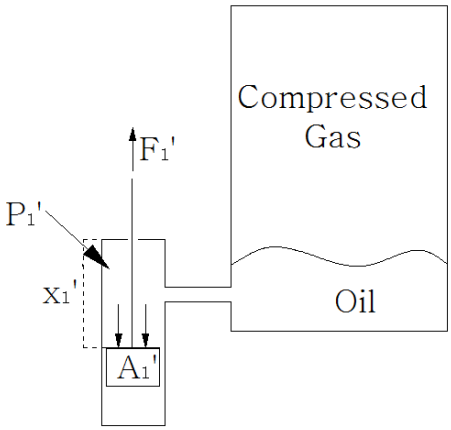

Figure 29. Hydro-pneumatic spring

A hydro-pneumatic spring can also do the same job. This kind of spring has a bladder as a separation element comprising oil and gas. Since oil can take more pressure than gas, the hydro-pneumatic spring can produce a bigger constant force in a more compact structure with smaller dimensions (Figure 29), compared with the pneumatic spring. The pressure that the spring can supply can reach up highly to 200 bars. Moreover, the spring allows charging and discharging at a high frequency. Oil is practically incompressible therefore cannot store pressure energy. The compressed gas is utilized in the bladder for storing energy. The oil in the bladder is connected to the hydraulic circuit so that the bladder accumulator can draw or release oil during work.

4. Discussion and Conclusions

This paper shows how to design a balancing system for an articulated robot. After the dynamic analysis, the position of the balancing system and the design of spring parameters are discussed. As examples, two variants of an articulated robotic structure are equipped with proper balancing systems. Both links of the robot are balanced by means of different springs and auxiliary devices. For the first structure, numerical examples show the balancing effect when the positions of the springs are different and the springs are provided with constant or variable forces. For a constant-force case, the robot can be approximately statically balanced with low-stiffness mechanical springs or pneumatic springs. For a variable-force case, the perfect balance is realized through the spring design and the torque error only depends on the orientation α_5 (or α_6), regardless of the ratio. For the second structure, pulley, cable and cross mechanisms, (hydro-) pneumatic springs compose the balancer. Pneumatic, and hydro-pneumatic springs are discussed for torque compensation.

There are pros and cons between the two variants. For the first structure, the robot with a parallelogram has a limited workspace. Motors and the balancing system mounted on the base give the robot more elasticity. For the second structure, the direct drive on joint makes the second link of the robot bulky and increase the mass and inertia. With pulley and cable mechanism, the robot has wider workspace. The load on the end effector is also taken into consideration when the static gravity is balanced.

For robotic structures with 3 DOF, the third degree of freedom which axis is parallel to the gravity vector need not to be considered in the robotic static balance. Therefore, the static balance of spatial industrial robots in this situation is also included in this paper.

According to the methodology presented in this paper, articulated robots can be perfectly statically balanced in all configurations. This paper shows a feasible way to design balancing devices and define their parameters based on considerations of practical requirements. This paper considers the two structures of an articulated robots since they are widely applied in industry. Future work should focus on articulated robots with multi-degrees of freedom and dynamic response of robot equipped with balancing system. Also other robotic structures with prismatic pairs should be discussed as an extended application of the methodology shown in this paper.

References

[1] Annual Energy Review 2011. U.S. Department of Energy's Energy Information Administration. DOE/EIA-0384(2011), September, 2012.

[2] Bruzzone L, Bozzini G. Energetic efficiency of a statically balanced hybrid industrial manipulator. In: Proceedings of 9th international workshop on research and education in Mechatronics, Bergamo, Italy, 2008.

[3] Hamza D. Effect of mass balancing on the actuator torques of a manipulator. Mech. Mach. Theory, 1995, 30(4): 495-500.

[4] Bruzzone L, Bozzini G. Elastic Balancing of a SCARA-Link Hybrid Industrial Manipulator, In: Proceedings of 28th IASTED International Conference Modelling, Identification and Control (MIC 2009), Innsbruck, Austria, 2009.

[5] Hervé, J. Device for Counter-Balancing the Forces Due to Gravity in a Robot Arm, 1985, Patent No. FR2565153.

[6] Baradat C., Arakelian V., Briot S., Guegan S. Design and prototyping of a new balancing mechanism for spatial parallel manipulators. Journal of Mechanical Design, 2008, 130: 072305.

[7] Segla S., Kalker-Kalkman, Schwab. Statically balancing of a robot mechanism with the aid of a genetic algorithm. Mech. Mach. Theory, 1998, 33: 163-174.

[8] Saravanan R., Ramabalan S., Badu P. Optimum static balancing of an industrial robot mechanism. Engineering Application of Artificial Intelligence, 2008, 21.

[9] Rizk R., Krut S., Dombre E. Design of a 3D Gravity Balanced Orthosis for Upper Limb, In: Proceedings of IEEE International Conference on Robotics and Automation, 2008.

[10] Streit, D.A., Shin. E. Equilibrators for Planar Linkages, J. Mech. Des., 1993, 115(3): 604-610.

[11] Streit, D.A., Shin. E. An Energy Efficient Quadruped with Two-Stage Equilibrator, J. Mech. Des. 1993, 115: 156-163.

[12] Lens T., Stryk O. Investigation of Safety in Human-Robot-Interaction for a Series Elastic, Tendon-Driven Robot Arm, In: Proceedings of the IEEE-RSJ International Conference on Intelligent Robots and Systems (IROS), 2012.

[13] Morita T., Kuribara F., Shiozawa Y. A Novel Mechanism Design for Gravity Compensation in Three Dimensional Space, In: Proceeding of the 2003 IEEE/ASME International Conference on Advanced Intelligent Mechatronics, 2003.

[14] Hain, K. 'Force Analysis', 'Spring Mechanism-Point Balancing' and 'Spring Mechanisms-Continuous Balancing', Spring Design and Application, Chironis, N. P., McGraw- Hill, New York, 1961, 268-275.

[15] Ion S., Liviu C. The static balancing of the industrial robot arms Part I: Discrete balancing. Mech. Mach. Theory. 2000, 35: 1287-1298.
[16] Ion S., Liviu C. The static balancing of the industrial robot arms Part II: Continuous balancing. Mech. Mach. Theory. 2000, 35: 1299-1311.
[17] Sunil. A, Abbas F. Gravity-balancing of Classes of Industrial robots, In: Proceedings of the 2006 IEEE International Conference on Robotics and Automation, May, 2006.
[18] Sunil K., Abbas F. Gravity-balancing of spatial robotic manipulators. Mech. Mach. Theory. 2004, 39: 1331-1344.
[19] Sai K., Sunil K., Abbas F., et al. Gravity-Balancing Leg Orthosis and Its Performance Evaluation. IEEE Trans. Robot. 2006, 22: 6.
[20] Mathijs V., Martijn W. Intrinsically safe robot arm: Adjustable static balancing and low power actuation. Int J Soc Robot, 2010, 2: 275-288.
[21] Nathan U., Vijay K. Passive mechanical gravity compensation for robot manipulators. In Proceedings of IEEE international conference on robotics and automation, Sacramento, California, April 1991.
[22] Just L. Herder. Design of spring force compensation systems Mech. Math. Theory 1998, 33: 151-161.
[23] Gabrielle J.M., Just L. Herder. Design, actuation and control of an anthropomorphic robot arm. Mechanism and Machine Theory, 2000, 35: 945-962.
[24] Herder, J. L. Energy-Free Systems: Theory, Conception and Design of Statically Balanced Mechanisms. Ph.D. thesis, Delft University of Technology, 2001.
[25] Tsai, L. W. Robot Analysis: The mechanics of Serial and Parallel Manipulators, Wiley-Intersecience Publication, John Wiley and Sons, 1999.
[26] Quaglia G., Yin Z. Optimization of static balancing for an anthropomorphic robot. In: Proceedings of the 3rd IFToMM International Symposium on Robotics and Mechatronics, Singapore, October, 2013.
[27] Quaglia G., Yin Z. A Balancing Mechanism for An Anthropomorphic Robot. Advanced Materials Research 2003, 774-776:1397-1403.
[28] Shin E., Streit D.A. Spring equilibrator theory for static balancing of planar pantograph linkages. Mechanism and Machine Theory, 1991, 26: 645-657.
[29] Clément M. Gosselin. Gravity compensation, static balancing and dynamic balancing of parallel mechanisms, in Smart Devices and Machines for Advanced Manufacturing, edited by Lihui Wang and Jeff Xi, Springer, London, England.
[30] Sami Haddadin, Alin Albu-Schäffer and Gerd Hirzinger. Requirements for Safe Robots: Measurements, Analysis and New Insights. The International Journal of Robotics Research. Vol. 28, No. 11–12, 2009: 1507–1527.
[31] Walsh G.J., Streit D.A. and Gilmore B.J. Spatial Spring Equilibrators Theory. Mech. Mach. Theory. Vol. 26, pp. 155-170, 1991.
[32] Streit D.A., Gilmore B.J., Perfect Spring Equilibrators for Rotatable Bodies. ASME Journal of Mechanisms, Transmissions, and Automation in Design, Dec, Vol. 111, pp. 451-458, 1989.
[33] Jieguo Wang, Clément M. Gosselin. Static balancing of spatial four-degree-of-freedom parallel mechanisms. Mech. Mach. Theory. Vol. 35, 2000: 563-592.
[34] Jieguo Wang, Clément M. Gosselin. Static balancing of spatial three-degree-of-freedom parallel mechanisms. Mech. Mach. Theory. Vol. 34, 1999: 437-452.
[35] Andrea Russo, Rosario Sinatra, Fengfeng Xi. Static balancing of parallel robots. Mech. Mach. Theory. Vol. 40, 2005: 191-202.
[36] G.G. Lowen, F.R. Tepper, R.S. Berkof. Balancing of linkages – an update. Mech. Mach. Theory. Vol. 18, 1983: 213-220.

[37] Hong-Sen Yan, Ren-Chung Soong. Kinematic and dynamic design of four-bar linkages by links counterweighing with variable input speed. Mech. Mach. Theory. Vol. 36, 2001: 1051-1071.